平成 29 年度三重大学大学院生物資源学研究科修士論文

台風の衰弱過程～圏界面変動の影響～

Weather and Climate Dynamics Division Graduate school of Bioresources Mie University

516M202 Jumpei Kanai *Supervisor*: Prof. Yoshihiro Tachibana

Feburary 28, 2018

Abstract

Some tropical cyclones (TCs) generated in North Pacific approach Japan in decay period. It is common that almost all of TCs decay through factor of cold sea surface temperature, landfall, and wind shear. However, some TCs decay due to unknown factor without them. It is important for Japanese to recognize unknown factor of decay fully in order to predict behavior of TCs.

MERRA reanalysis have been used to investigate the tropical cyclones (TCs) via peculiar decay in North Pacific summer for the period 1980 – 2015. As a result of examination, 10 TCs is extracted. Their composite indicates upper-level warming just before decay.

In order to investigate the TC decay mechanism, Winnie (in 1997) is selected and simulated. In contrast to many TCs generated in the north Pacific, TC Winnie in 1997 started to decay in the subtropics, which is atypical among the TCs in north Pacific. In order to investigate this peculiar behavior of the TC, a numerical simulation was conducted as well as the analysis of the ERA-Interim data. A distinctive warm air was found near the tropopause around the TC center during the decaying phase of the TC. The upper-level warm air is reported, but how height warm air make TCs weakened. The results of this study, we suggest the new factor of weakness that warm air near tropopause lead to the TC decay via the static stability by the downward motion of the tropopause.

Contents

1. Introduction

Tropical cyclones (TCs) generated over the North Pacific Ocean approach to Japan every year. According to Japan Meteorological Agency, strength of TCs generally reach peak or decay stage when they locate within 300km of Japan every year. Although some TCs develop anomalously and frequently cause a disaster by heavy precipitation in Japan, a large number of TCs weakens before arriving at the Japan. In the past several decades, many previous studies addressed to clarify a mechanism of TCs genesis or development to predict limit disaster damage but TCs decay was not paid much attention such as TCs genesis or growth. Recently a demand of weather prediction is increasing not only for human activity such as a disaster prevention but also economic community to expect output of clean energy and to control costs of logistics, according to Weather Business Consortium (WXBC). To control our economic or prevention activity efficiently, we need predictability of TCs. For improving the predictability of TCs, we must understand mechanisms about genesis, development, and decay.

A one factor for influence to TCs intensity, which includes development and decay, is sea surface temperature (SST). Evans (1993) suggested that intense tropical cyclones were found over waters warmer than another threshold temperature, $28℃$. Kuroda et al. (1998) also showed storms of higher relative intensity have been over warmer waters for a day or two prior to the observation time than those of lower relative intensity. It was also mentioned that TCs intensity is greatly influenced by the cold water over which the TC moves. Other factors related with TCs weakening, Paterson et al. (2005) shows wind shear value greater than $10\ \mathrm{m\ s^{-1}}$ are associated with weakening, with values greater than $12\mathrm{ms^{-1}}$ favoring rapid weakening. Jones et al. (2003) shows factor of weakness is included making landfall, cold sea surface temperature (SST), wind shear. Although these factors, which are SST, vertical wind shear, and landed over the ground, apparently dominates the weakening of TCs intensity, some TCs staying over the North Pacific Ocean are rapidly decaying under the condition that is not identified these factors. For examples, TC Winnie observed August in 1997 decay rapidly on North Pacific Sea with wind shear less than 10m/s and high SST. Therefore, there is some possibility that unknown factor inside of the TC may make that weakened.

We suggest the new factor of weakness. The process is below

1) The downdraft induced by microphysics heating forms upper-level warming.

2) The upper-level warm air stabilize tropopause air column

3) Upper –level stabilization make convection of TC weakened and as a result, TC intensity is weakened.

The upper-level warm air is reported some studies on the basis of simulation [Persing and Montgomery 2003; Chen and Zhang 2013; Wang and Wang 2014]. It is known that the process of upper-level warming is due to the total advection associated with subsidence from the lower stratosphere into the eye [Ohno and Satoh 2015]. However, it is unknown whether the height of the warm-core maximum is related to the intensity of TCs.

In this study, we focus on warm air near tropopause. At first, in order to investigate the relationship between upper-level warm air and TCs intensity, we extract TCs decaying peculiarly without factor of landfall, cold SST, wind shear and ascertain whether composite of them show warm air near tropopause. Secondarily, as the representative of extracted TCs, we focus on TC Winnie in 1997. As mentioned above, Winnie is good case of decay without factor of landfall, cold SST, wind shear. To investigate relationship between upper-level warm air and intensity in detail, we use numerical simulation. Finally, we conduct sensitivity experiment which restrain upper-level warming and investigate the warm air contribute to TC decay. The results in this study show upper-level warm air control TC intensity.

2. Data and Method

2.1. Data

In order to investigate TCs intensity and track, 6 hourly TCs minimum central pressure(MCP) and track data on the North Pacific Ocean were extracted from Japan Meteorological Agency for the period 1980 – 2015 and focus on summer which is between July to September.

To examine environment surrounding TCs, SST data is used National Oceanic and Atmospheric Administration (NOAA) Optimum interpolation sea surface temperature (OISST, daily), which resolution is 0.25° ×0.25° [Reynolds et al., 2002]. Modern-Era Retrospective analysis for Research and Applications (MERRA) is also used in this study [Rienecker et al., 2011].

2.2. Method

a. Extraction method of composite members

To extract TCs through decay without factor of cold SST, landfall, wind shear, conditions is defined below

(1) Decaying rapidly in North Pacific area

We extract TCs that MCP rate of change in North Pacific area between $0^{\circ} - 30^{\circ}\mathrm{N}$, $120^{\circ} - 150^{\circ}\mathrm{E}$ is less than -2σ. MCP rate of change is defined as $MCP(t + 24\mathrm{hr}) - MCP(t)$, where *t* is time. MCP rate of change greater than zero means intensification, less than zero means decay.

(2) Weak wind shear

We extract TCs with wind shear less than 10m/s. Wind shear is calculated as a vector difference between the 200- and 850-hPa wind, averaged over a 20°

latitude-longitude square on the TCs center.

(3) Warmer SST

We extract TCs on which SST is more than 50% tile, where the SST was used 12hour before TCs decay at the point.

As a result, we can extract 10 TCs.

To confirm structure of extracted TCs, we calculate composite as below respectively,

C1: Extracted 10 TCs

TCs decay without cold SST, landfall, wind shear.

C2: All of TCs through decay.

TCs with MCP rate of change below zero.

C3: Contractive TCs

Intensity retain below 920hPa for 24 hours.12 TCs is extracted as contractive TCs.

We compare C1 with C2 and C3 to investigate structure of TCs through peculiar decay.

b. Numerical simulation

In order to investigate TC structure in detail, this study use Weather Research and Forecasting (WRF) model Version 3.4.1 [Skamarock et al., 2008]. The outermost domain (d01) have horizontal resolution of 50km. The second outside domain (d02) have that of 10km. d01 area is set in $116^{\circ}-167^{\circ}\mathrm{E}, 2^{\circ}-37^{\circ}\mathrm{N}$ and d02 is set in $128^{\circ}-140^{\circ}\mathrm{E}, 19^{\circ}-30^{\circ}\mathrm{N}$, respectively. Both domains included 80 vertical layer and top is 10hPa. As physics options, we select WRF Single Moment 6-class scheme as microphysics. Longwave radiation physics is RRTMG scheme and shortwave radiation is RRTMG shortwave. Noah Land Surface Model is used as Land surface physics. MM5 similarity is used as surface layer. Also, Kain-Fritsch scheme is used as cumulus parameterization in d01 only. European Centre for Medium-Range Weather Forecasts (ECMWF) reanalysis (ERA-interim) data is inserted as the initial and lateral boundary condition [Simmons et al., 2007]. The span of this experiment is 10day from 10 to 20 August 1997. We analysis during 15 to 18 August to investigate around peak intensity.

To investigate the relationship between upper-level warm air and TC intensity, this study conduct two contrasting experiment. One is standard experiment (CTL) and the other is that only temperature rate of up between σ=56 (near 12.6km height) to σ=75 (near 25.8km height) height is cut by 70 % from august 14rd in not order to develop warm air near tropopause considerably (COLD). Compering two experiment, we investigate the impact that warm air at tropopause changes TC intensity.

3. Results

3.1. Structure of TCs through peculiar decay

Figure 1 shows tracks and weak points of extracted 10 TCs respectively. 10 TCs proceed toward northwest and near $20^{\circ}-25^{\circ}$N, TCs is weakened. Likewise, MCP transitions of 10 TCs, which are intensified and weakened rapidly, is similar (Figure 2). This result indicates that extracted TCs are similar behavior and 10 TCs go through significant decay. Figure 3 shows the static stability of 10 TCs and composite. In this study, the static stability is defined as difference of air temperature subtracting at 400hPa height from 200hPa near TCs center. Just before decay, the static stability is rapidly increased about 2 K/day on 10TCs average. At that time, temperature of 10 TCs is warmer at 200hPa than other all of TCs (Fig. 4).

To compare structure of 10TCs to 12 TCs, longitude-pressure height cross section of difference of temperature standardized for TCs surroundings between composite of 10 TCs and 12 TCs at 0hour, 24hour ago 48hour ago, respectively(Fig. 5). Near 200hPa pressure height at TCs center, 10TCs is warmer than 12TCs at 0 hour and 24hour ago. But at 48hour ago, 10TCs near 200hPa are colder. Figure 6 shows static stability of 12TCs. It shows that Static stability of 12TCs is down just before 0hour contrasting to 10TCs (Fig. 4). Investigating relationship of TCs intensity and static stability, large static stability correspond to weak intensity (Fig. 7).

Past several studies, warm air is reported, however, it is unknown whether the height of the warm-core maximum is related to the intensity of TCs [Ohno and Satoh 2015]. We suggest the peculiarity of 10 TCs is that warm air exist near tropopause.

3.2. Standard experiment

In order to investigate the relationship between upper-level warm air and TC intensity in detail, we use WRFv3.4.1 and simulate TC Winnie (in 1997), which is representative of extracted 10 TCs. Figure 8 indicates MCP of both actual and simulation value. In simulation, Winnie intensified until 06:00 UTC on 16 August at 24.53°N, 136.54°E. Although there is time difference of intensity change between simulation and actuality, intensity transition is well reproduced in simulation. Figure 9 shows SST at 18:00 UTC on 16 August in simulation. SST is more 301K at location where Winnie decaying. Also, Wind shear is under 10m/s which value is not enough to make TC weakened (figure not shown). Figure 10 shows outgoing longwave radiation (OLR) at 06:00 on 16 August in simulation and Figure 11 shows real infrared image at decay (06:00 on 13 August), respectively. In simulation, the eye is formed as similar to actual. As will be described later, warm air near 16km height develop in decay period , as same as composite of 10 TCs.

From the above, Winnie at the decay stage is well reproduced in the simulation. Therefore, simulated result is examined in detail. In this simulation, intensification period (IP) is defined from 06:00 UTC on 15 August to 06:00 UTC on 16 August and decaying period (DP) is from 06:00 UTC on 16 August to 06:00 UTC on 17 August.

Figure 12 shows radius-height cross section of the temperature difference between DP and IP, which is azimuthally averaged as respect to the center of the TC. Temperature of the DP near 16km height at a radius of approximately 100km is warmer. To understand the mechanism that upper-level warm air is formed, we confirm difference of adiabatic heating near 16km. It is apparent that difference near 16km height is not large (Fig.13). Figure 14 shows potential vorticity (PV) and potential temperature of latitude and longitude cross sections on the basis of the TC center each period of intensification and decay. PV is given by

$$\mathrm{PV} \equiv \frac{1}{\rho} \zeta_\theta \cdot \frac{\partial \theta}{\partial p} \qquad (1)$$

where ρ is density; ζ_θ is absolute vorticity on isentropic surface; θ is potential temperature; and p is pressure. PV unit is defined as pvu [$10^{-6}\mathrm{m}^2\mathrm{s}^{-1}\mathrm{Kkg}^{-1}$] [Hoskins et al., 1985].

Distribution of potential temperature is compatible with that of potential vorticity well at upper-level height and fall to troposphere more considerably in decay period. Figure 15 shows radius-height cross section of the radial and vertical wind at IP and DP respectively. It is apparent in the figure that in radial wind flow into the eye and downward flow at upper-level in DP is stronger.

Figure 16 shows time-height Hovmöler plot of the PV averaged at storm center, where the storm center is defined as range of 100km from TC center. It indicates that upper-level PV descends to the tropopause. It is considered that air in stratosphere presses into the TC. Figure 17 shows the time-height Hovmöler plot of the temperature anomaly from the time-average at the storm center. At approximately 03:00 UTC on August, We notice that warm air appear near 16km height just before TC decay. Corresponding to the upper-level warm air develop at 16km height, updraft is weakened in tropopause (Figure 18).

3.3. Sensitivity experiment

From the above analysis, upper-level warm air appears just before the TC decaying. In order to make the impact of upper-level warm air effect clearly, we make comparison between CTL and COLD run. Figure 19 shows sea level pressure (SLP) of CTL and COLD run at 06 on 16 August. It's apparent that SLP difference between CTL and COLD run is not large. It means the change of upper-level heating rate is not enough to have impact to distribution of SLP. Also, transitions of vertical wind shear of both simulations are similar (Figure 20).

Figure 21 shows MCP of CTL and COLD run. Despite of similar surroundings, the TC simulated by COLD run is more intensified. Figure 22 shows the time-height Hovmöler plot of the temperature comparison between CTL and COLD run. Near 16km height, temperature in CTL run is warmer. Corresponded with upper-level warmer air from 00:00UTC on 16 August to 06:00UTC on 17 August, PV is larger in CTL run (Fig.23). For upper-level warmer air and higher PV in CTL run, updraft is weakened (Fig. 24). Therefore, we suggest that relationship between upper-level warm air and TC intensity.

4. Discussion and Conclusion

We examined TCs through peculiar decay in the North Pacific for the period 1980 – 2015 on summer. As a result, we could extract 10 TCs. To confirm structure of 10 TCs, we compare C1 with C2, C3 respectively. Upper-level temperature in 10 TCs was warmer than others just before TCs decay. Also, the upper-level warm air appeared and static stability increased just before decay. The results implied it was in condition that updraft was easily restrained and weakened. In fact, when upper-level static stability was large, the TCs intensity tend to weaken.

To examine the relationship between Upper-level warm air and intensity in detail, a numerical experiment was conducted using WRFv3.4.1. This study, object case of numerical simulation was Winnie (in 1997), which locates on highest SST and simulated.

To investigate the mechanism of upper-level warm air, Potential temperature and potential vorticity were calculated. Potential temperature was compatible with potential vorticity well at upper-level height and fall to troposphere more considerably in DP. From the fact that downdraft was also stronger in DP near 16km height, upper-level warm air was formed by upper-level circulation. The process of upper-level warm air was mentioned by (Ohno and Satoh 2015).

To investigate correspondence upper-level warm air and intensity, we saw time series at storm center. Time-height Hovmöler plots of the PV and temperature showed that upper-level PV and temperature descended to the TC. Immediately after the temperature deviation was net value, updraft is weakened. This was considered that upper-level warm air forced TC convection weakened. Because it was difficult to remove other factor controlling TC intensity without upper-level warming, we conducted sensitivity experience. Comparing CTL and COLD run, TC intensity in CTL run, which has upper-level warm air, was more weakened, Corresponded with the intensity difference, updraft was more weakened in CTL run. The difference between CTL and COLD run was similar to the DP in CTL run.

From the above results, we suggest new process of TC intensity decay. The new process is below.

1) The downdraft induced by microphysics heating forms upper-level warming.

2) The upper-level warm air stabilize tropopause air column

3) Upper –level stabilization make convection of TC weakened and as a result, TC intensity is weakened.

Acknowledgment

I express gratitude to Professor Tachibana, my supervisor. He taught me the basic knowledge of the physics. I appreciate to him.

I express gratitude to associate Prof Atuyoshi Manda. He taught me the knowledge of WRF simulation, sensitive experiment, and detailed knowledge of the physics the atmospheric dynamics. Additionally, he support me with various aspects. I appreciate to him with deepest gratitude.

Kazuaki Nishii taught me the statistical analysis about TCs. Moreover, he taught me logical thinking about study very hard. I really appreciate to him.

Koji Yamazaki taught me the knowledge of the physics and typhoon. I appreciate to him.

Many professors of Geosystem Science, Graduate school of Bioresources, Mie University advised me. I thank that very much.

Many professors of Institute for Space-Earth Environmental Research of Nagoya University taught me the detailed knowledge of Typhoon. I thank that very much.

Members of climate and ecosystems dynamics laboratory provided some advices for my research. I was helped by their advises. I express gratitude to them.

References

Chen, H., and D.-L. Zhang,2013: On the rapid intensification of Hurricane Wilma (2005). Part II: Convective burstd and the upper-level warm core. *J.atoms. Sci*., **70**, 146-162, doi:10.1175/JAS-D-12-062.1.

Evans, J.L., 1993: Sensitivity of tropical cyclone intensity to sea surface temperature. *J. Climate*, **6**,1133-1140.

Hoskins, B. J., M. E. McIntyre, and A. W. Robertson, 1985: On the use and significance of isentropic potential vorticity maps. *Quart. J. Roy. Meteor. Soc*., **111**, 877-946

Jones, S., P.A. Harr, J. Abraham, L. F. Bosart, P. J. Bowyer, J. L. Evans, D. E. Hanley, B. N. Hanstrum, R. E. Hart, F. Lalaurette, M. R. Sinclair, R. K. Smith, and C. Thorncroft, 2003 : The extratropical transition of tropical cyclones, *Weather and Forecasting,* **Vol18**, 1052-1092.

Kuroda, M., A. Harada, and K. Tomine, 1998: Some aspects on sensitivity of typhoon intensity to sea-surface temperature. *J. Meteor. Soc. Japan*, **76**, 145-151.

Ohno, T., and M. Satoh, 2015: On the warm core of a tropical cyclone formed near the tropopause. J. ***Atmos. Sci*., 72,** 551-571

Paterson, L. A., B. N. Hanstrum, N. E. Davidson, and H. C. Weber, 2005: Influence of environmental vertical wind shear on the intensity of hurricane-strength tropical cyclones in the Australian region. *Mon. Wea. Rev*.**, 133**, 3644-3660

Persing, J., and M. T. Montgomery, 2003; Hurricane superintensity. *J. Atmos. Sci*., **60,** 2349-2371. doi:10.1175/1520-0469(2003)060,2349:HS.2.0.CO;2.

Reynolds, R.W., N.A. Rayner, T.M. Smith, D.C. Stokes, and W. Wang, 2002: An improved in situ and satellite SST analysis for climate. *J. Climate,* **15**, 1609-1625.

Rienecker, M.M., M.J. Suarez, R. Todling, J. Bacmeister, E. Liu, M.G. Bosilovich, S.D. Schubert, L. Takacs, L. Takacs, G.-K. Kim, S. Bloom, J. Chen, D. Collins, A. da Silva, et al. 2011 : MERRA: NASA's Modern-Era Retrospective Analysis for Research and Applications, *Journal of Climate*, **Vol 24**, 3624-3648.

Simmons, A., S. Uppala, D. Dee, and S. Kobayashi, 2007: ERA-Interim: New ECMWF reanalysis products from 1989 onwards. *ECMWF Newsletter*, **110,** 25–35.

Skamarock, W. C. et al., A Description of the Advanced Research WRF Version 3. Vol. 113 (*NCAR Technical Note* NCAR/TN-475+STR, 2008).

Wang, H., and Y. Wang, 2014: A numerical study of Typhoon Megi(2010): Part I: Rapid intensification. *Mon. Wea. Rev.,* **142**, 29-48, doi:10.1175/MWR-D-13-00070.1.

Figure captions

Figure 1. Tracks and weak points of extracted 10 TCs. X marks location of TC weakened.

Figure 2. MCP [hPa] of 10 TCs. Center line show the time TCs start decay and drawn ±240hour.

Figure 3. Static stability [K] of 10 TCs at storm center. As a reference decay, drawn during ±215hour. Gray line indicates MCP of 10 TCs respectively and back line is composite of them.

Figure 4. Longitude-pressure height cross section of difference between composite of 10 TCs and all. The difference is that temperature is standardized for TCs surroundings respectively and subtracted composite of all of TCs from 10 TCs.

Figure 5. Longitude-pressure height cross section of difference between composite of 10 TCs and 12TCs. The difference is that temperature is standardized for TCs surroundings respectively and subtracted composite of 12 TCs from 10 TCs. a)0hour b)24hour ago c)48hour ago respectively.
0hour is the time TCs start decay in C1 and TCs reach 920hPa in C3, respectively.

Figure 6. Static stability [K] of 12 TCs at storm center. As a reference decay, drawn during ±215hour. Gray line indicates MCP of 12 TCs respectively and back line is composite of them.

Figure 7. Scatter plot of static stability[K] at 0hour and MCP[hPa] at 12hour later. Blue circle means 10 TCs and pink circle means 12 TCs. Blue star shows 10 TCs average and red star shows 12 TCs average.

Figure 8. MCP [hPa] of both actual (black line) and simulated (red line). Upper time axis is actual and bottom is simulated.

Figure 9. SST [K] in simulation at 18:00 on 15 August. Black line is track and TC symbol is decay location at 06:00 on 16 August.

Figure 10. OLR [W/m^2] at 06:00 on 16 August in simulation.

Figure 11. Real infrared image at decay (06:00 on 13 August).

Figure 12. Radius-height cross section of temperature difference [K] by subtracting IP from DP.

Figure 13. Radius-height cross section of microphysics latent heating [m/s].

Figure 14. (a) latitude in IP, (b) latitude in DP, (c) longitude in IP and (d) longitude in DP –vertical cross sections respectively. Color is PV [pvu] and contour is potential temperature [K].

Figure 15. Radius-height cross section of the radial wind [m/s] in (a) IP and (b) DP and vertical wind in (c) IP and (d) DP, respectively.

Figure 16. Time-height Hovmöler plot of the PV [pvu] at storm center.

Figure 17. Time-height Hovmöler plot of the temperature anomaly [K] from time-average at the storm center.

Figure 18. Time-height Hovmöler plot of the vertical wind [m/s] at the storm center.

Figure 19. SLP [hPa] of CTL (red line) and COLD (blue line) run at 06 on 16 August.

Figure 20. Vertical wind shear [m/s] of CTL (red line) and COLD (blue line) run, respectively.

Figure 21. MCP [hPa] of CTL (red line) and COLD (blue line) run.

Figure 22. Time-height Hovmöler plot of the temperature difference [K] subtracting COLD from CTL run at storm center.

Figure 23. Time-height Hovmöler plot of the PV difference [pvu] subtracting COLD from CTL run at storm center.

Figure 24. Time-height Hovmöler plot of the vertical wind difference [m/s] subtracting COLD from CTL run at storm center.

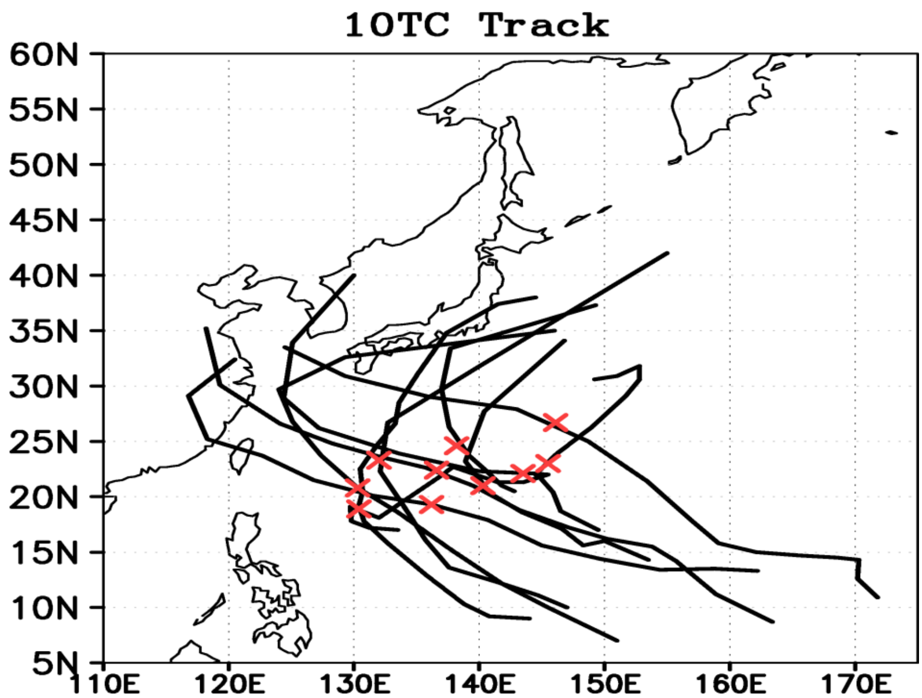

Figure 1. Tracks and weak points of extracted 10 TCs. X marks location of TC weakened.

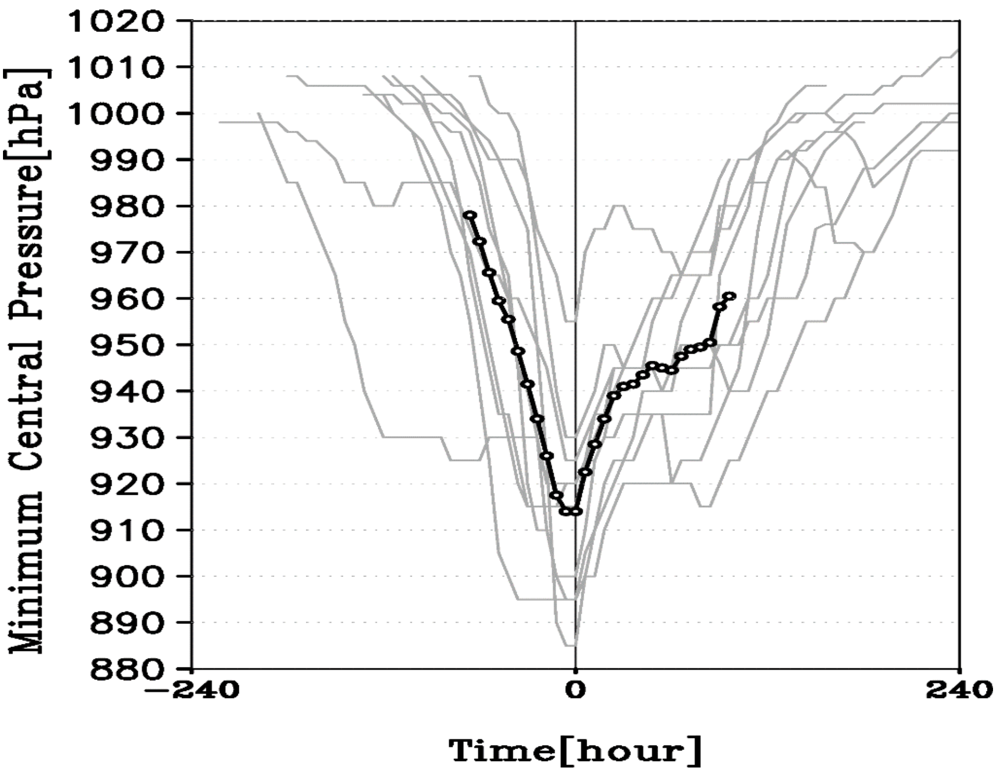

Figure 2. MCP [hPa] of 10 TCs. Center line show the time TCs start decay and drawn ±240hour.

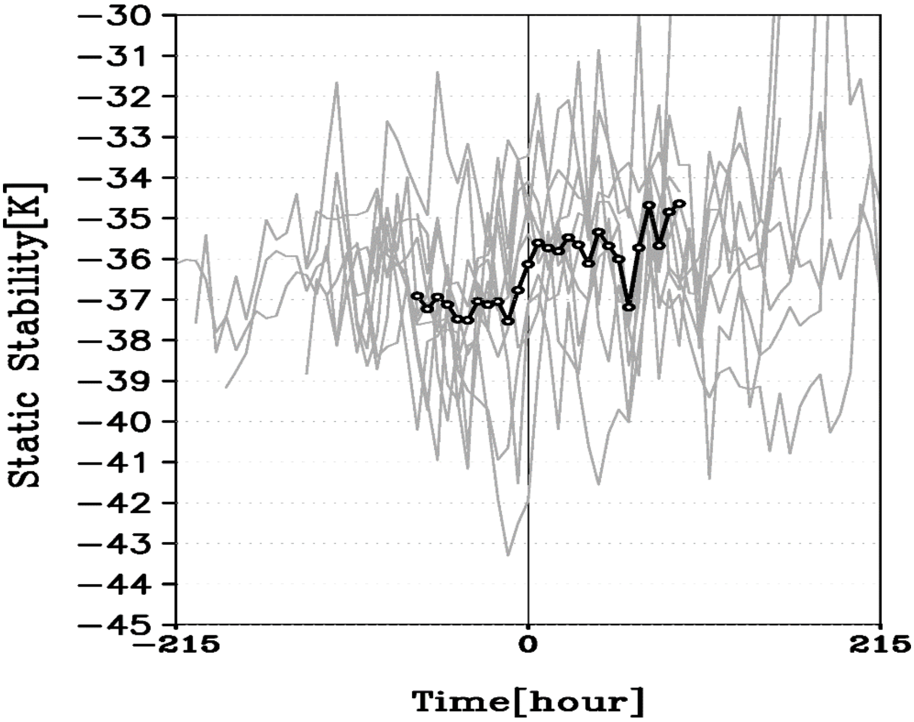

Figure 3. Static stability [K] of 10 TCs at storm center. As a reference decay, drawn during ±215hour. Gray line indicates MCP of 10 TCs respectively and back line is composite of them.

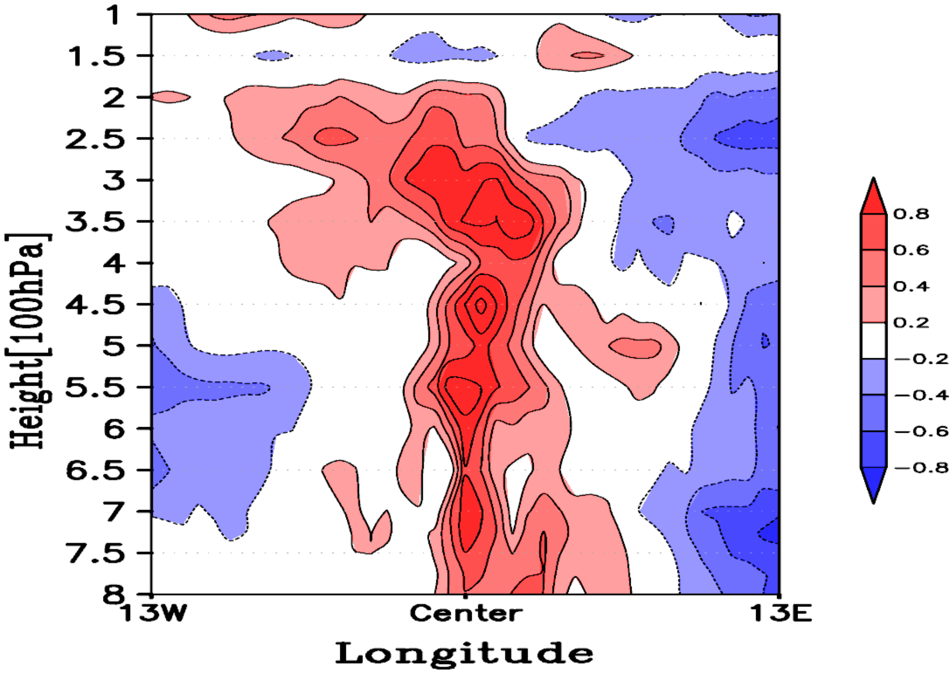

Figure 4. Longitude-pressure height cross section of difference between composite of 10 TCs and all. The difference is that temperature is standardized for TCs surroundings respectively and subtracted composite of all of TCs from 10 TCs.

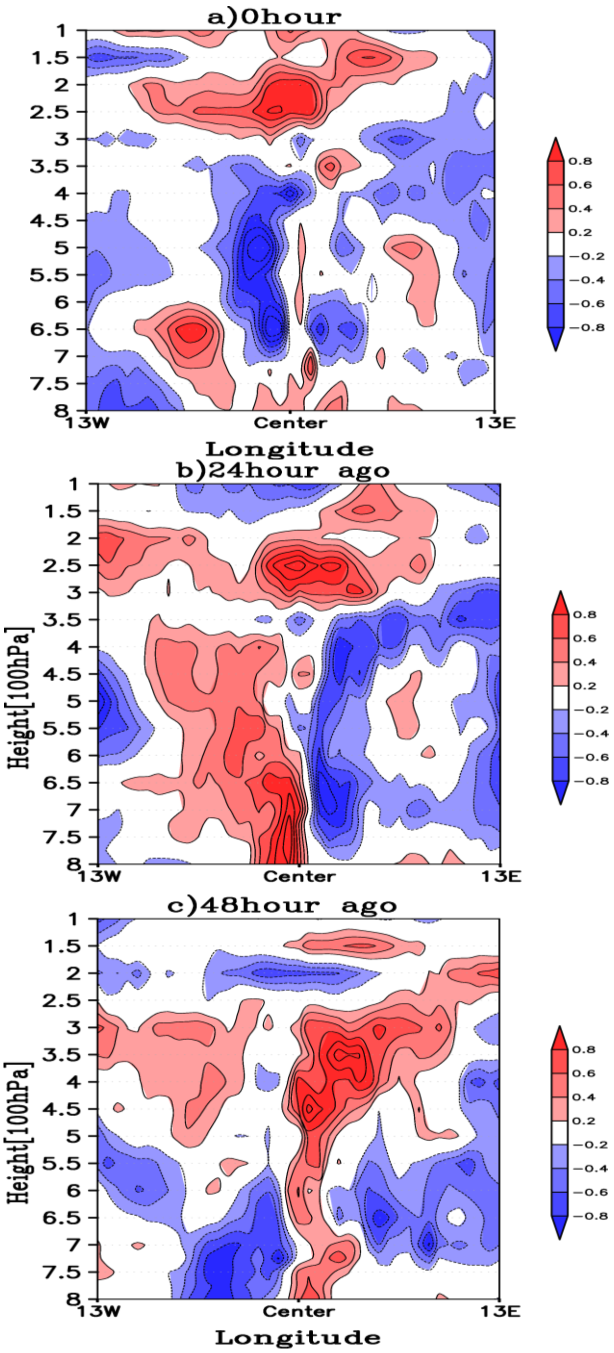

Figure 5. Longitude-pressure height cross section of difference between composite of 10 TCs and 12TCs. The difference is that temperature is standardized for TCs surroundings respectively and subtracted composite of 12 TCs from 10 TCs.

a)0hour b)24hour ago c)48hour ago respectively.

0hour is the time TCs start decay in C1 and TCs reach 920hPa in C3, respectively.

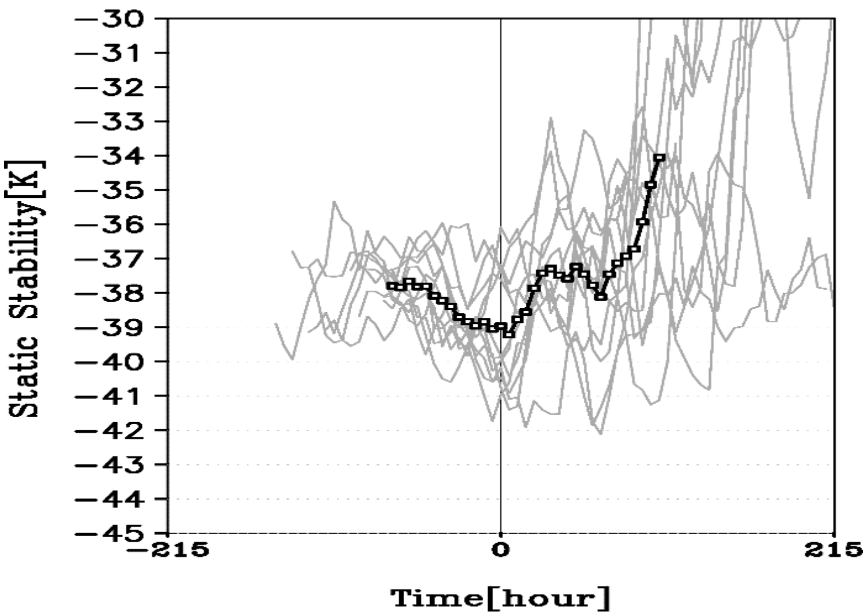

Figure 6. Static stability [K] of 12 TCs at storm center. As a reference decay, drawn during ±215hour. Gray line indicates MCP of 12 TCs respectively and back line is composite of them.

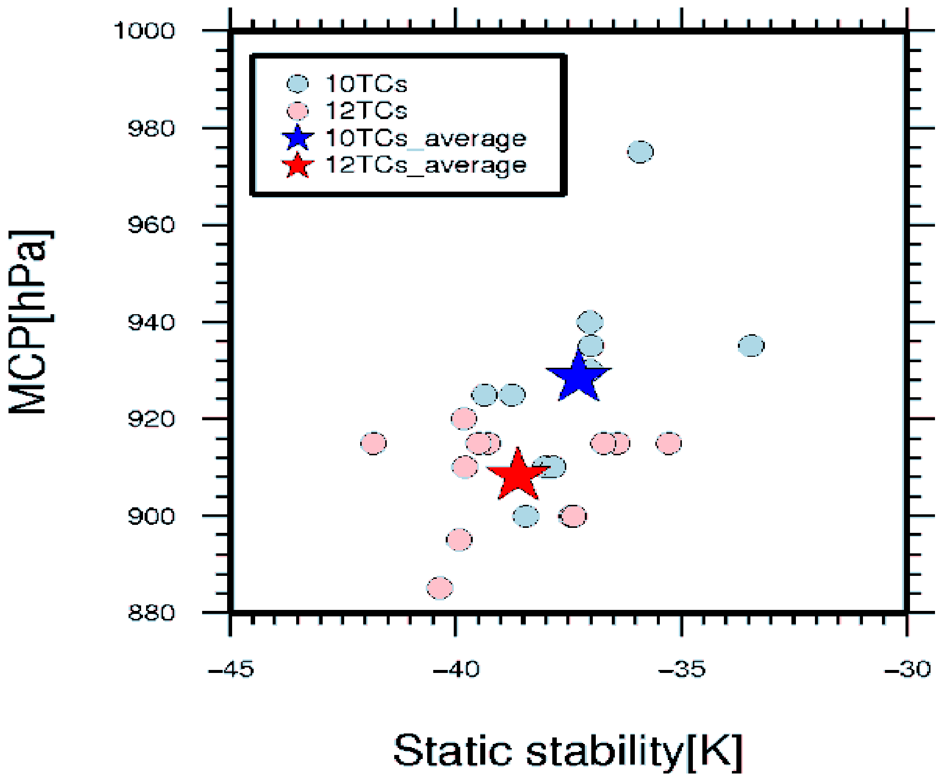

Figure 7. Scatter plot of static stability[K] at 0hour and MCP[hPa] at 12hour later. Blue circle means 10 TCs and pink circle means 12 TCs. Blue star shows 10 TCs average and red star shows 12 TCs average.

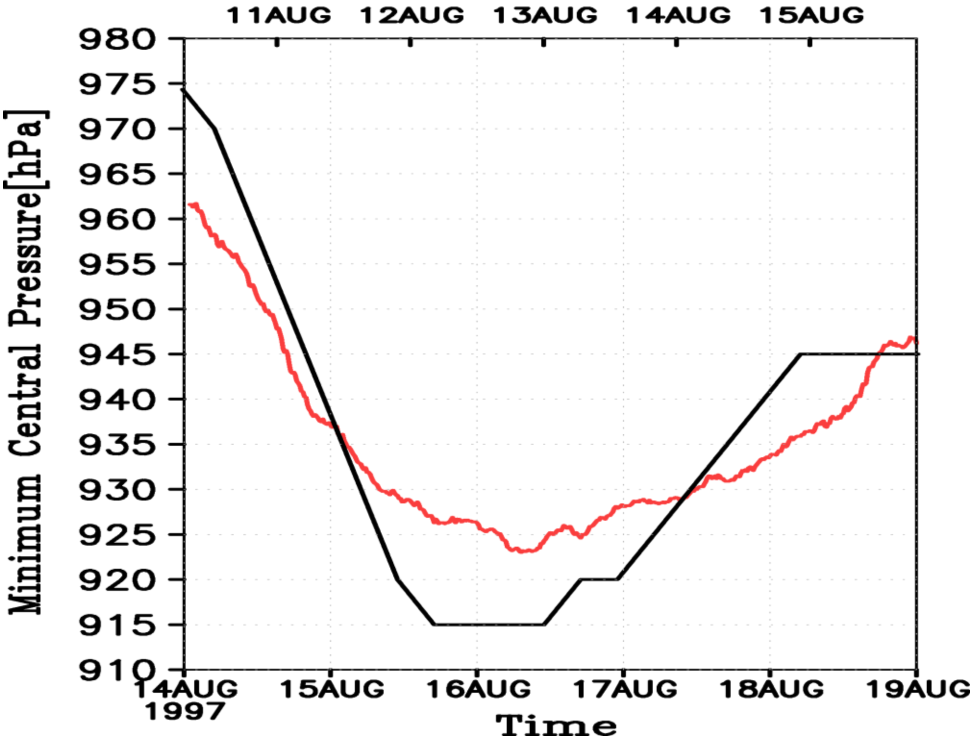

Figure 8. MCP [hPa] of both actual (black line) and simulated (red line). Upper time axis is actual and bottom is simulated.

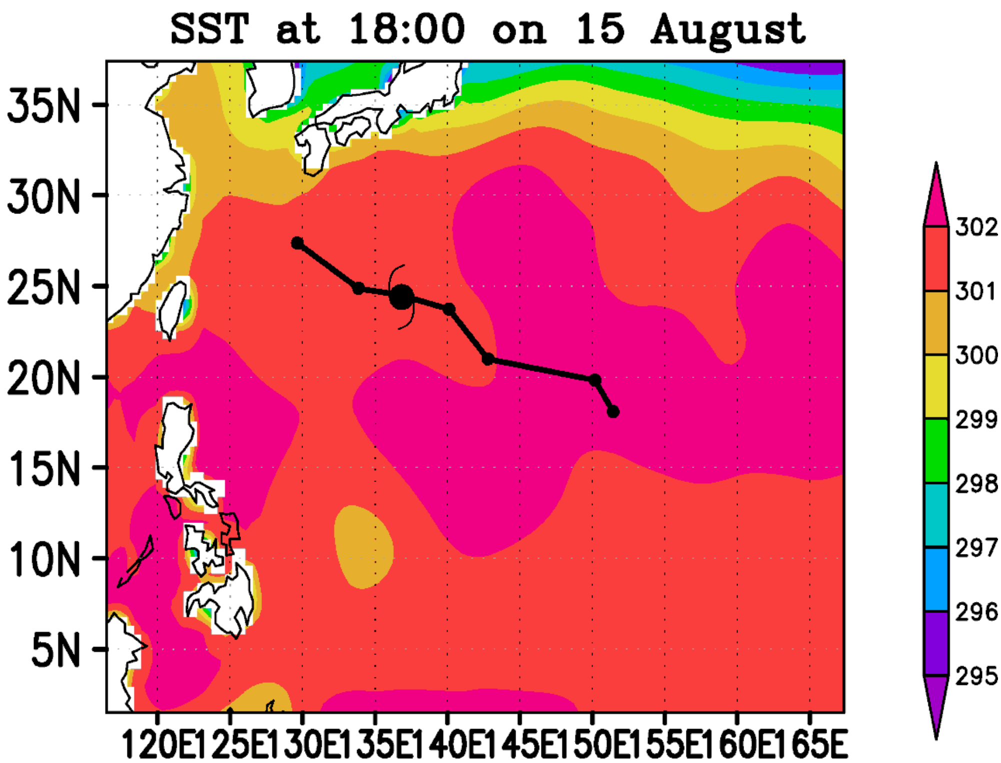

Figure 9. SST [K] in simulation at 18:00 on 15 August. Black line is track and TC symbol is decay location at 06:00 on 16 August.

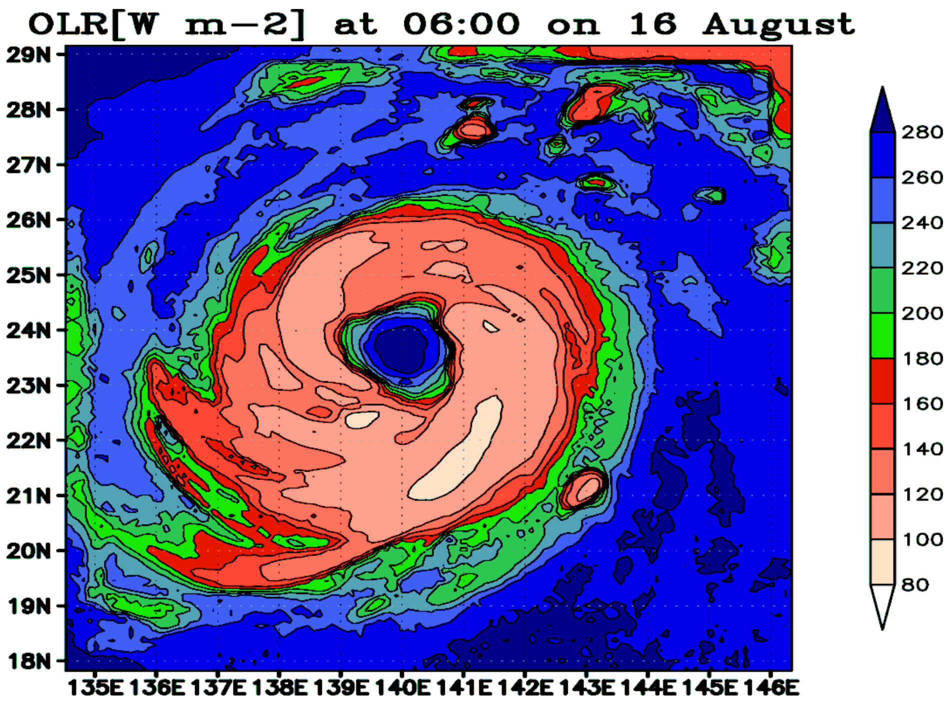

Figure 10. OLR [W/m^2] at 06:00 on 16 August in simulation.

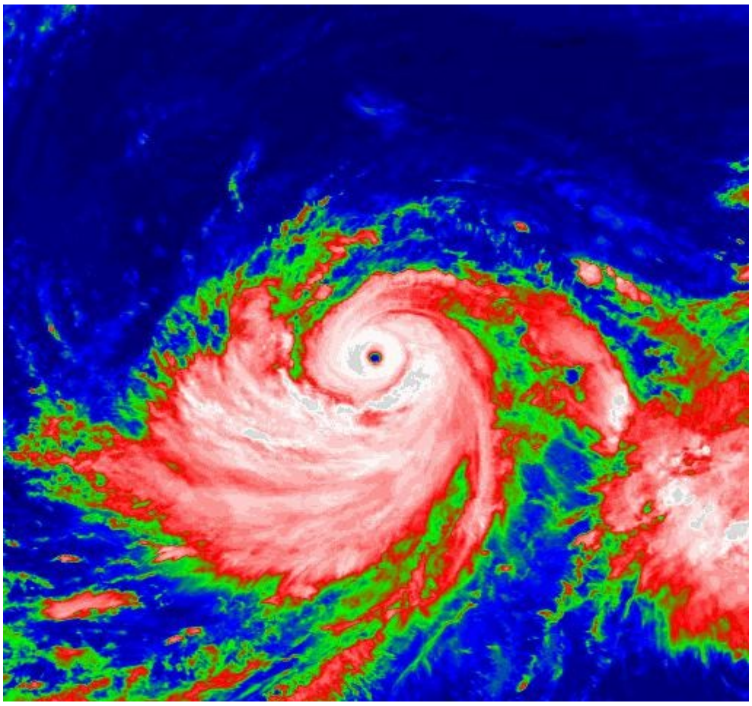

Figure 11. Real infrared image at decay (06:00 on 13 August).

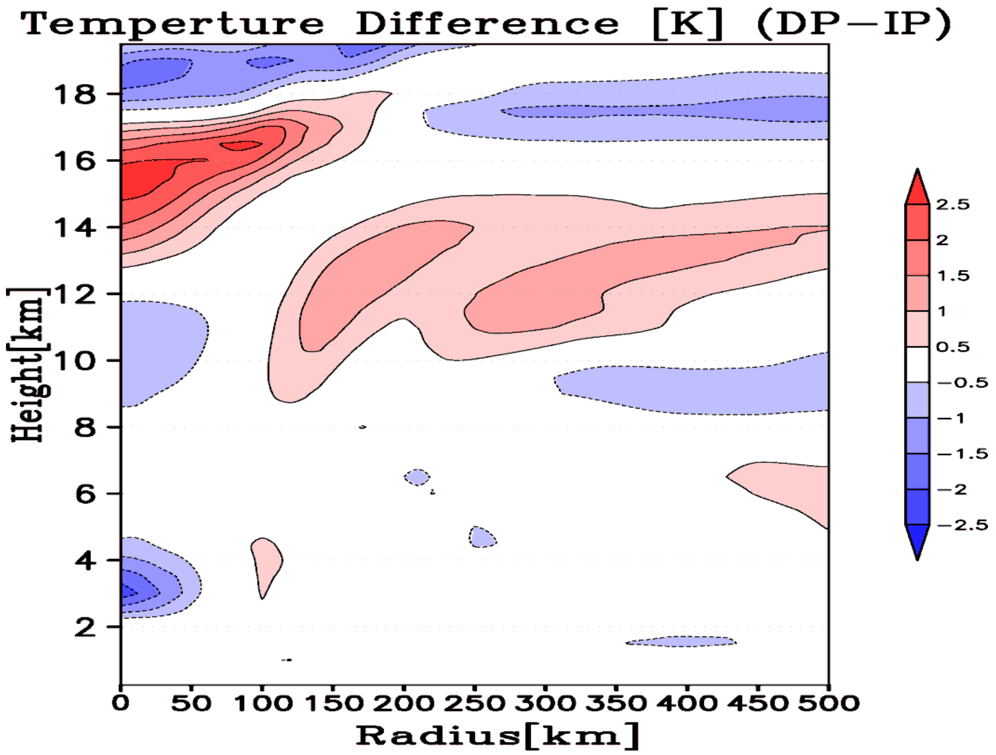

Figure 12. Radius-height cross section of temperature difference [K] by subtracting IP from DP.

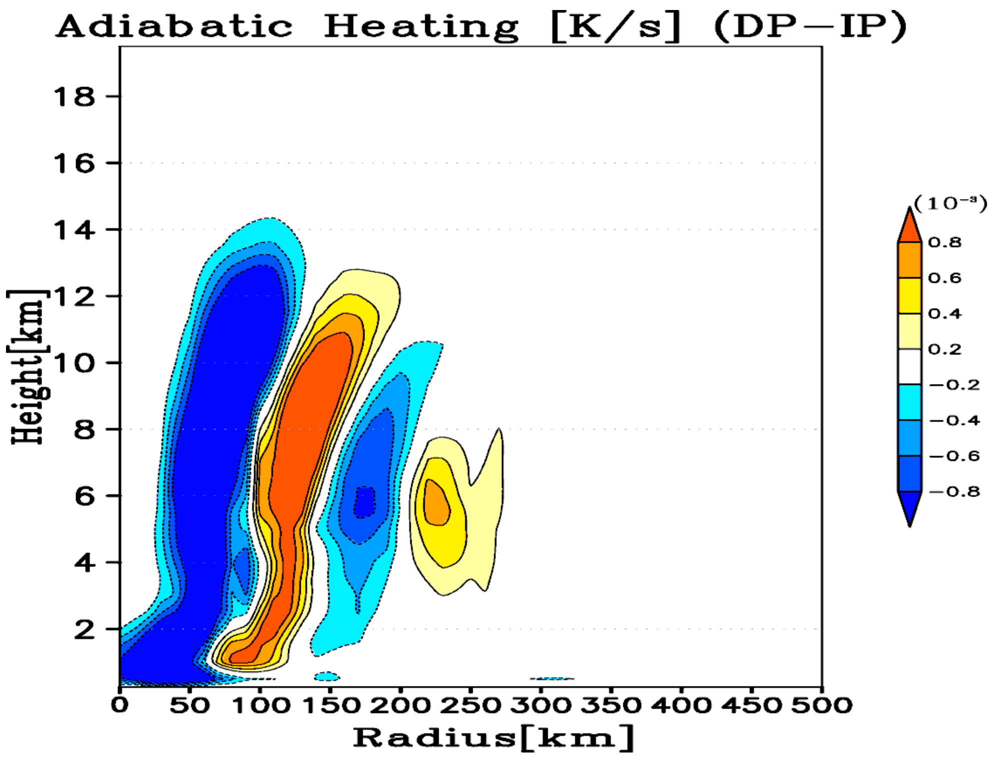

Figure 13. Radius-height cross section of microphysics latent heating [m/s].

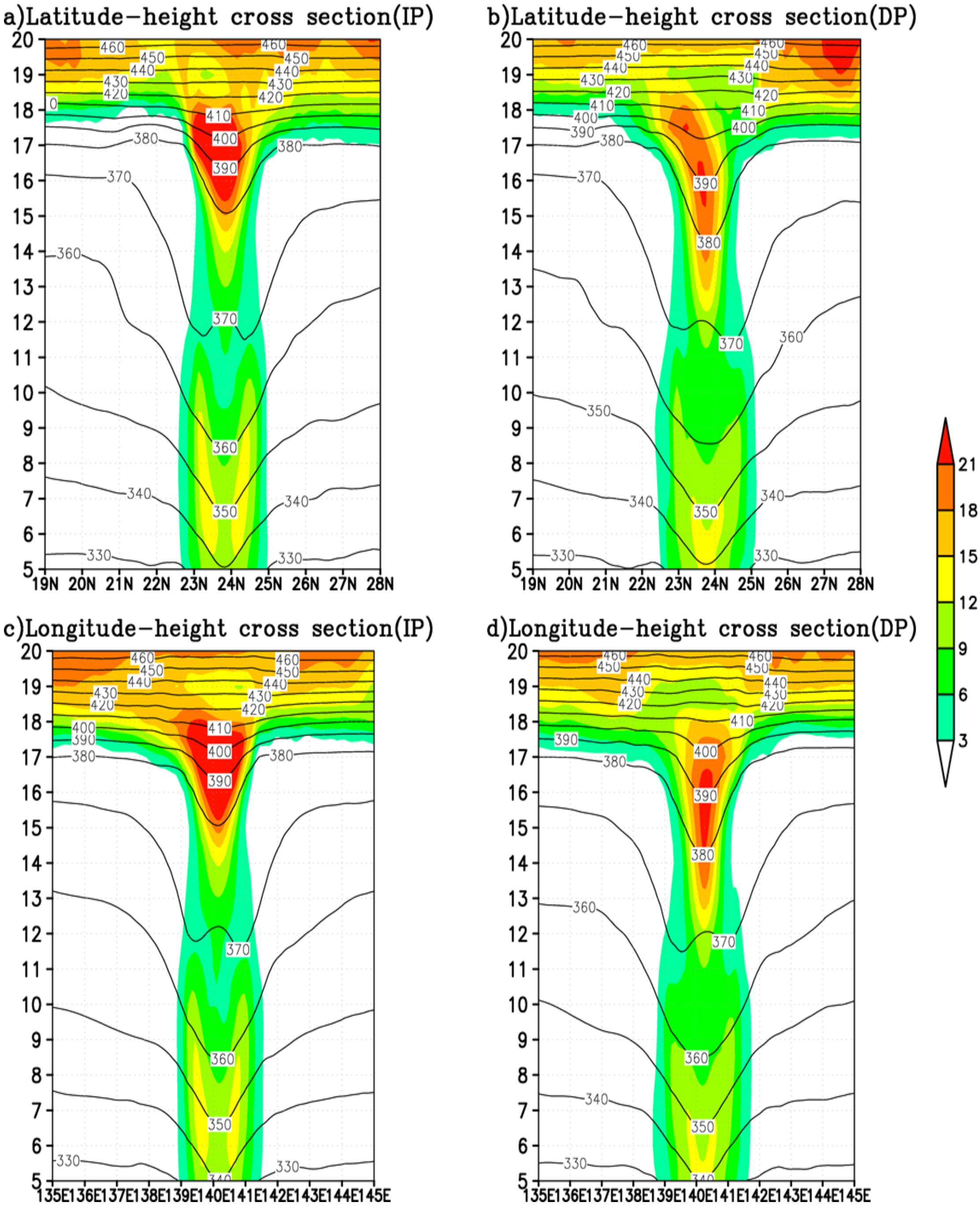

Figure 14. (a) latitude in IP, (b) latitude in DP, (c) longitude in IP and (d) longitude in DP –vertical cross sections respectively. Color is PV [pvu] and contour is potential temperature [K].

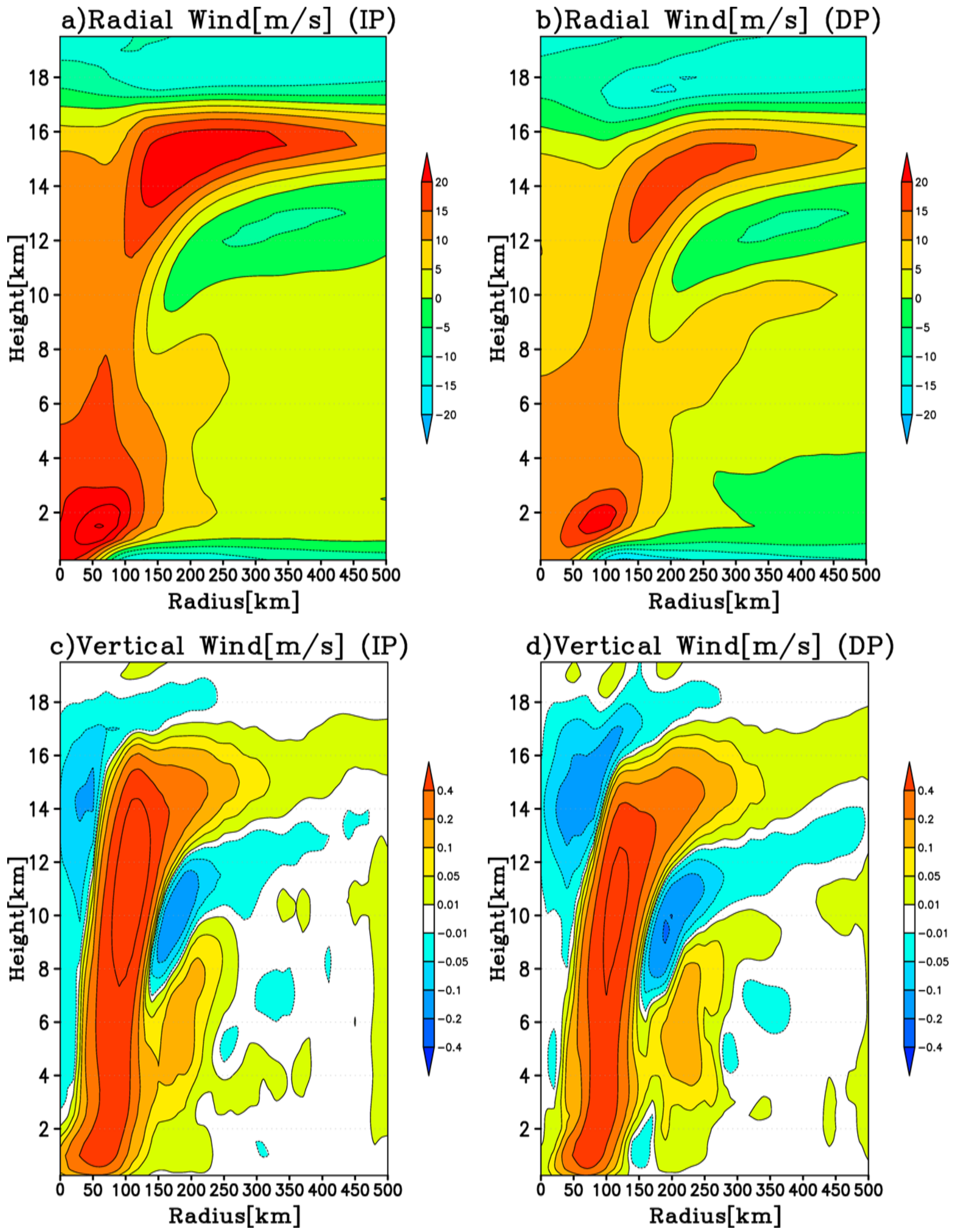

Figure 15. Radius-height cross section of the radial wind [m/s] in (a) IP and (b) DP and vertical wind in (c) IP and (d) DP, respectively.

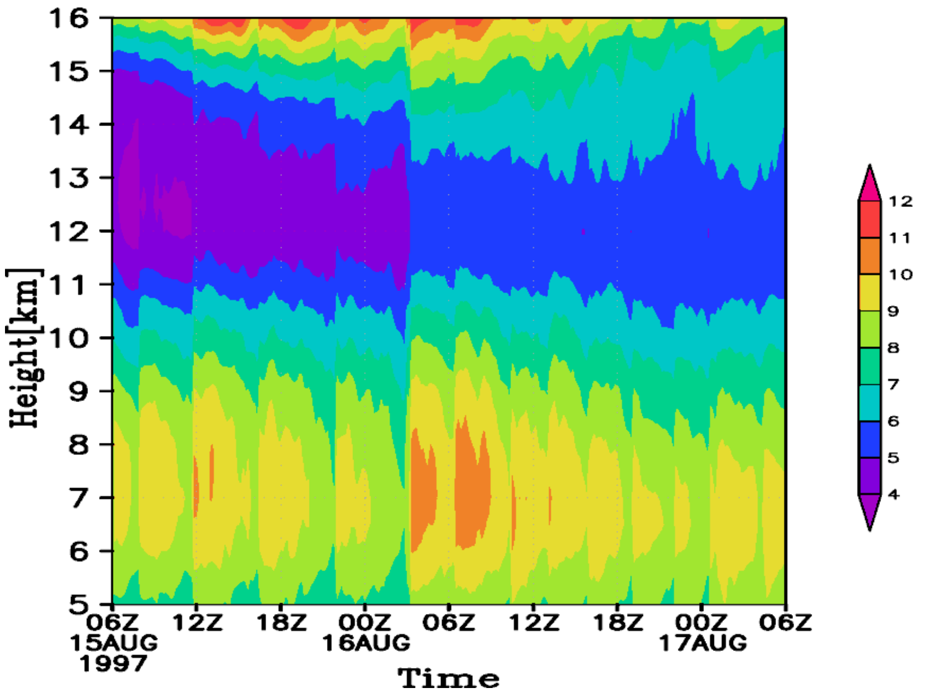

Figure 16. Time-height Hovmöler plot of the PV [pvu] at storm center.

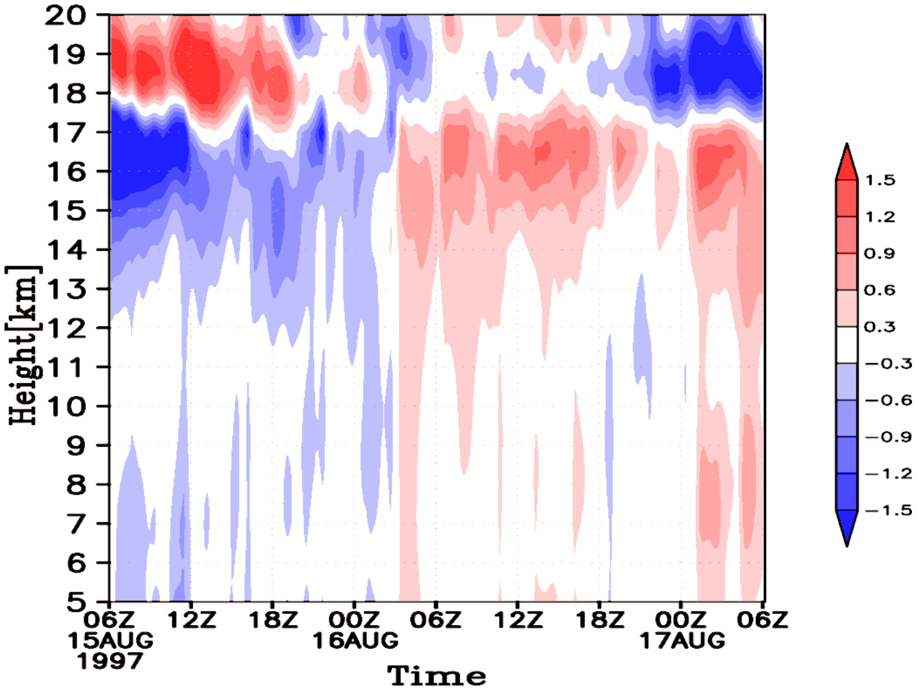

Figure 17. Time-height Hovmöler plot of the temperature anomaly [K] from time-average at the storm center.

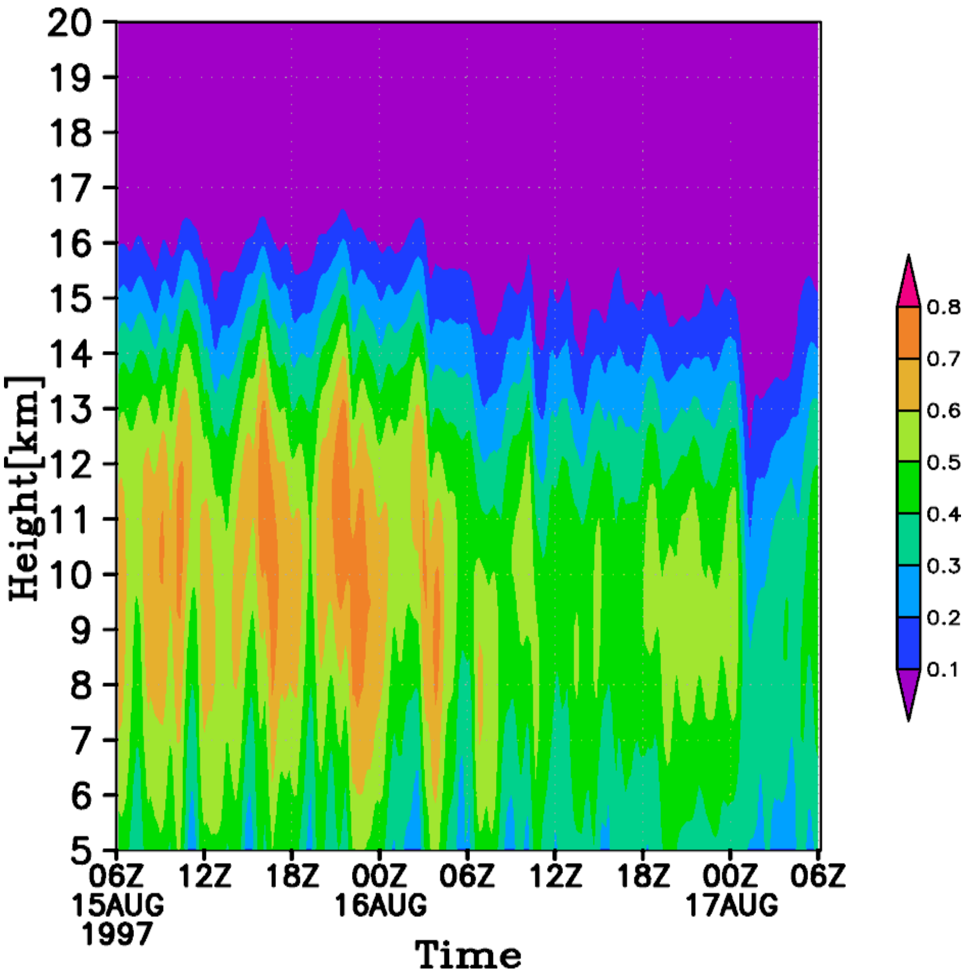

Figure 18. Time-height Hovmöler plot of the vertical wind [m/s] at the storm center.

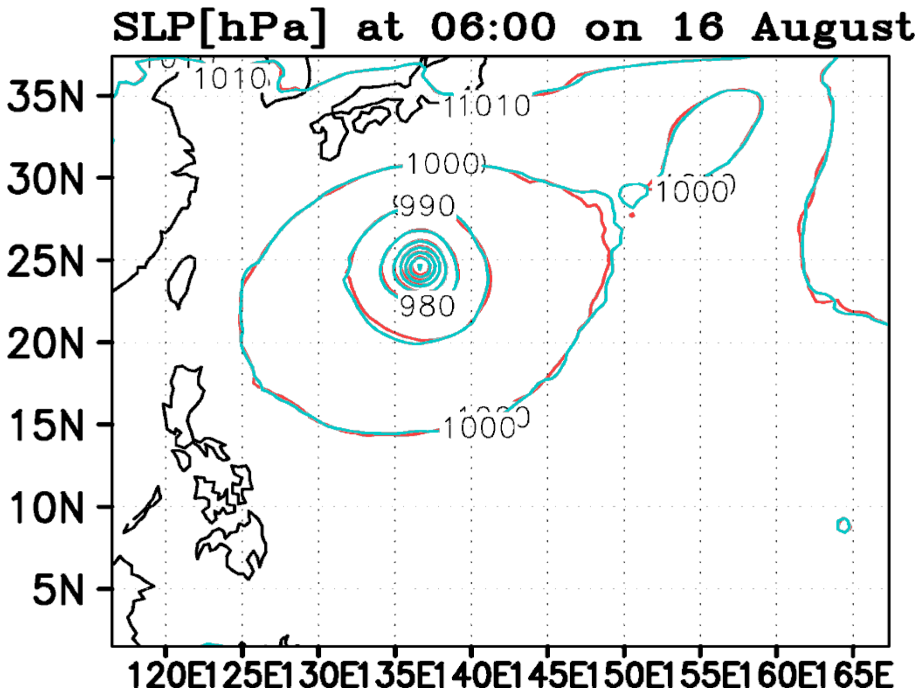

Figure 19. SLP [hPa] of CTL (red line) and COLD (blue line) run at 06 on 16 August.

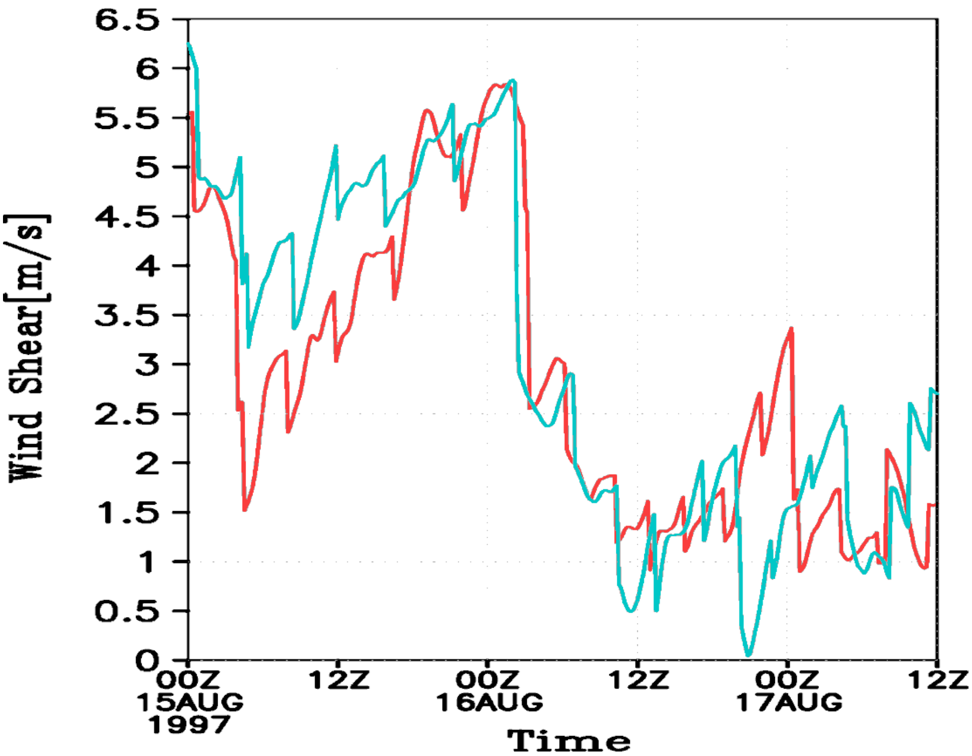

Figure 20. Vertical wind shear [m/s] of CTL (red line) and COLD (blue line) run, respectively.

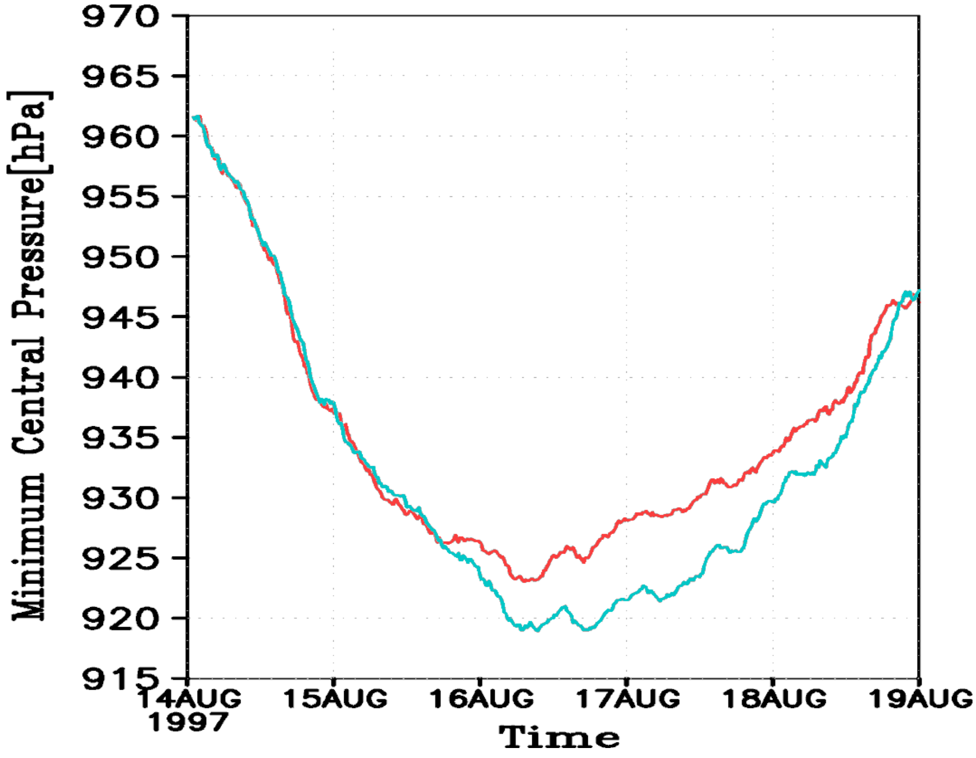

Figure 21. MCP [hPa] of CTL (red line) and COLD (blue line) run.

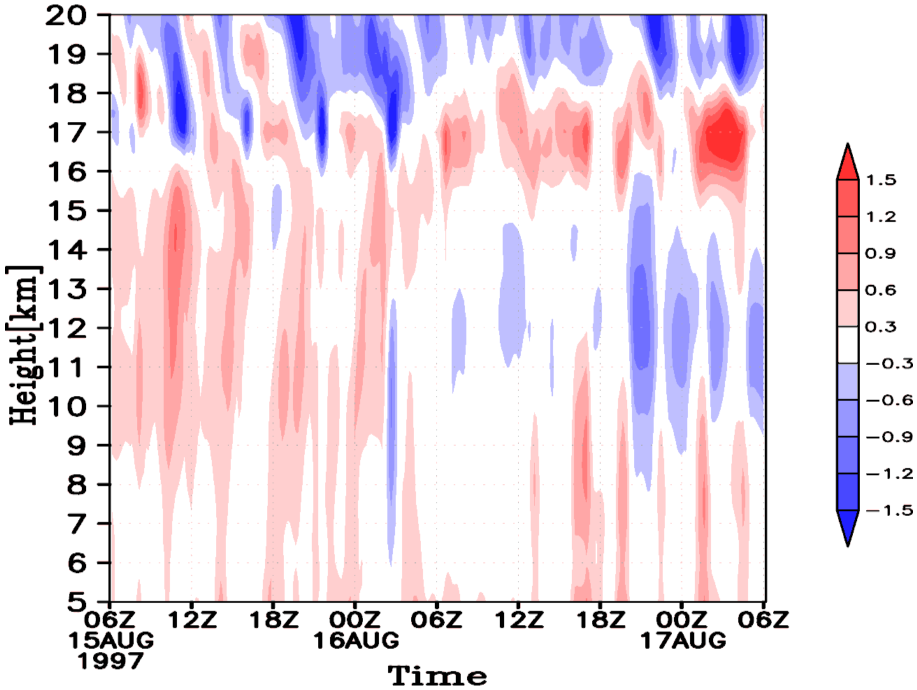

Figure 22. Time-height Hovmöler plot of the temperature difference [K] subtracting COLD from CTL run at storm center.

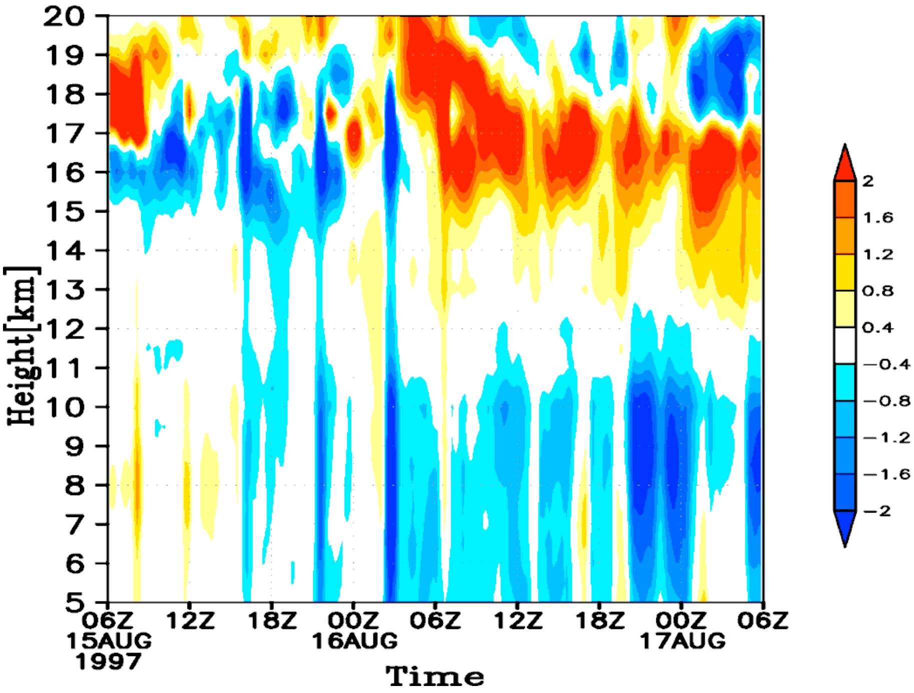

Figure 23. Time-height Hovmöler plot of the PV difference [pvu] subtracting COLD from CTL run at storm center.

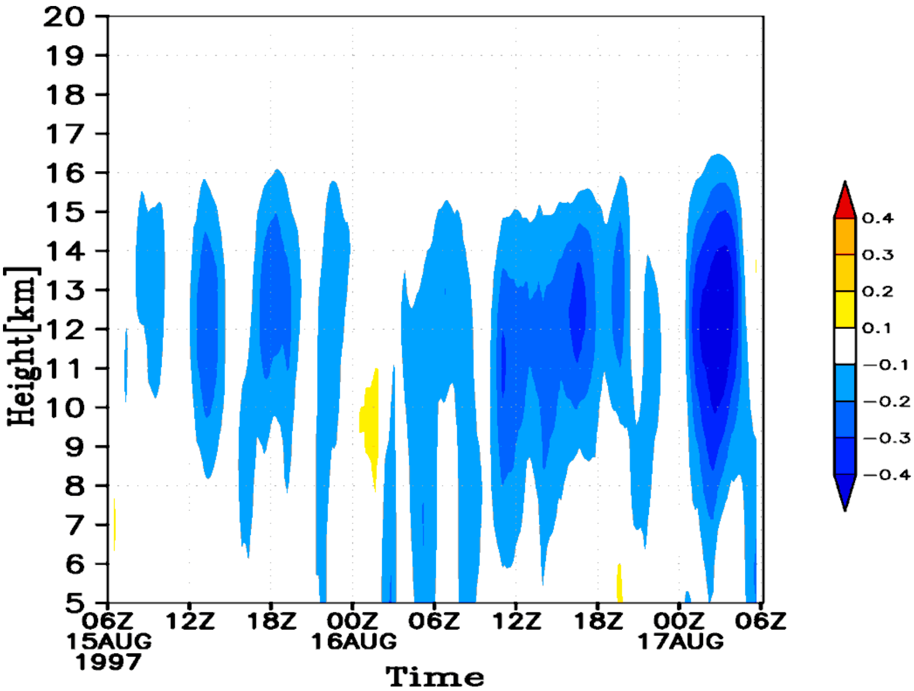

Figure 24. Time-height Hovmöler plot of the vertical wind difference [m/s] subtracting COLD from CTL run at storm center.